Chemical Amplification (or Dampening) of the Twomey Effect: Conditions Derived from Droplet Activation Theory

T. A. RISSMAN, A. NENES, AND J. H. SEINFELD

Departments of Chemical Engineering, and Environmental Science and Engineering, California Institute of Technology, Pasadena, California

ABSTRACT

Cloud droplet number concentrations are controlled by both meteorological and microphysical factors. Microphysical factors include aerosol number concentration and composition. This paper examines the importance of microphysical phenomena compared to the sensitivity with respect to parcel updraft velocity in the activation of aerosols to become cloud droplets. Of the compositional (chemical) factors that can influence droplet number concentration, the effect of organics is examined through their ability to alter droplet surface tension and to contribute solute. A recent parameterization of aerosol activation (by Abdul-Razzak et al.) is extended to obtain analytical expressions for the sensitivity of activation to microphysical factors relative to updraft velocity. It is demonstrated that, under some conditions, the droplet number concentration can be as much as 1.5 times more sensitive to changes in aerosol composition than to updraft velocity. Chemical effects seem to be most influential for size distributions typical of marine conditions and decrease in importance for strongly anthropogenically perturbed conditions. The analysis indicates that the presence of surface-active species can lead to as much uncertainty as results from variations in updraft velocity. The presence of surfactant species also drastically changes the response of the cloud condensation nuclei to changes in the updraft velocity spectrum. Conditions are found under which an increase in dissolved organic compounds can actually lead to a decrease in cloud droplet number, a ''contra-Twomey effect.'' Results presented have more general implications than just for organic compounds and can apply, in principle, for any chemically induced activation effect.

1. Introduction

Cloud optical properties depend on the in-cloud droplet size distribution, which, in turn, is controlled by the availability of atmospheric particles that serve as cloud condensation nuclei (CCN). Twomey (1977) suggested that an increase in aerosol number concentration from anthropogenic emissions, and thus an increase in CCN, would lead to a reduction in the size of cloud droplets and higher cloud albedo. This increase in cloud albedo, and the concomitant radiative cooling, is referred to as the first indirect climatic effect of aerosols (Houghton et al. 2001).

In assessing the importance of chemical variations in the composition of the CCN population, one has to compare the changes relative to dominant sources of variability, which are total aerosol number and updraft velocity. In doing so, a simple comparison of CCN spectra is not sufficient; droplet formation in clouds is a strongly nonlinear process, and the full process of activation needs to be considered for a correct treatment. Nenes

et al. (2002a) examined the effects of water-soluble gases, partially soluble species, surface-active species, and condensation kinetics on cloud droplet number concentration and, using a detailed numerical cloud parcel model, compared them with the Twomey effect. Their calculations show that, for a wide range of updraft velocities, chemical effects can rival those of the Twomey effect. The interaction for most cases is positive, indicating that chemical influences mostly act to enhance the Twomey effect. Given that organic compounds are ubiquitous in atmospheric aerosols, it is of interest to examine their influence on activation over the entire parameter space of organic mass fraction.

We propose here an extension of a parameterization to include surface tension effects consistent with Köhler theory (Abdul-Razzak et al. 1998; Abdul-Razzak and Ghan 2000). The modified parameterization is used to examine the sensitivity of the droplet number concentration to total aerosol number concentration, soluble organic mass fraction, and the geometric mean radius and geometric standard deviation of the aerosol size distribution using a normalized sensitivity ratio that compares the sensitivity to that of updraft velocity.

In the following sections, we present the derivation of the modified Köhler theory, which leads to an aerosol

---

Corresponding author address: Dr. J. H. Seinfeld, Departments of Chemical Engineering and Environmental Science and Engineering, CIT, Mail Code 210-41, Pasadena, CA 91125.
E-mail: seinfeld@caltech.edu

activation parameterization that includes surface tension effects; this will be referred to as the extended Abdul-Razzak, Ghan, and Rivera-Carpio (EAGR) parameterization. The EAGR parameterization is compared with a full, numerical adiabatic cloud parcel model to evaluate its performance in predicting the activation fraction. Sensitivities of cloud droplet number concentration to aerosol size distribution characteristics, organic content, and updraft velocity are then presented.

2. Analytical parameterizations of aerosol activation

Before proceeding, it is useful to present a brief overview of current aerosol activation parameterizations. Cohard et al. (1998) developed an activation parameterization based on a general description of the CCN spectrum, which depends on four parameters related to the aerosol size distribution characteristics, the solubility of the aerosol species, and the air temperature. They then used their activation parameterization to analyze the sensitivity of droplet number concentration to the geometric mean radius and the geometric standard deviation of single lognormal aerosol size distributions of marine and continental aerosols. Khvorostyanov and Curry (1999) assume the power-law aerosol size distribution of Junge (1952) to develop a simple expression relating CCN number concentration to supersaturation with parameters that are related to aerosol characteristics and growth dependence on relative humidity under subsaturation. Abdul-Razzak et al. (1998) and Abdul-Razzak and Ghan (2000) developed an aerosol activation parameterization involving both unimodal (Abdul-Razzak et al. 1998) and multimodal (Abdul-Razzak and Ghan 2000) lognormal aerosol size distributions.

The parameterizations of Abdul-Razzak et al. (1998) and Abdul-Razzak and Ghan (2000) are useful to investigate the sensitivity of droplet activation to both microphysical and dynamical factors because of the explicit link of updraft velocity and aerosol size distribution characteristics to droplet number concentration. The lognormal representation of the aerosol size distribution is also a desirable feature. However, these parameterizations lack explicit treatment of surface-active species. For these reasons, we include in the theory the effect of dissolved aerosol organics on droplet surface tension.

a. Köhler theory

Traditional Köhler theory predicts that the equilibrium saturation ratio for a droplet containing dissolved electrolytes and an insoluble core is (Seinfeld and Pandis 1998)

$$S - 1 = s = \frac{A}{r} - \frac{Ba_d^3}{r^3 - b_1 a_d^3}, \tag{1}$$

where S is the saturation, s is the supersaturation, A is

the curvature coefficient, r is the droplet radius, $B = (M_w \rho_{ap}/\rho_w)[(\varepsilon_s v_s/M_s) + (\varepsilon_o v_o/M_o)]$, $b_1 = \varepsilon_{ins} \rho_{ap}/\rho_{ins}$, $A = 2M_w \sigma_s/(RT\rho_w)$, a_d is the aerosol dry radius, M_w is the molar mass of water, ρ_{ap} is the density of the aerosol particle, ρ_w is the density of water, ε_s is the salt mass fraction, v_s is the number of ions resulting from the dissociation of one salt molecule, M_s is the molar mass of the salt species, ε_o is the dissolved organic mass fraction, v_o is the number of ions resulting from the dissociation of one organic molecule, M_o is the molar mass of the organic species, ε_{ins} is the insoluble mass fraction, ρ_{ins} is the density of the insoluble species, R is the gas constant, and T is the temperature. The density of the aerosol particle is given by

$$\rho_{ap} = \frac{1}{\dfrac{\varepsilon_o}{\rho_o} + \dfrac{\varepsilon_s}{\rho_s} + \dfrac{\varepsilon_{ins}}{\rho_{ins}}}, \tag{2}$$

where ρ_o is the density of the dissolved organic species and ρ_s is the density of the salt species.

The presence of dissolved organics can change the bulk phase surface tension of the droplet. Facchini et al. (1999) have proposed that the droplet surface tension, σ_s, can be expressed as a function of the dissolved organic concentration, C, by

$$\sigma_s = \sigma_s^* - A_1 T \ln(1 + A_2 C), \tag{3}$$

where σ_s^* is the surface tension of pure water, and A_1 and A_2 are constants. We will use this relationship to represent the change in surface tension from the presence of dissolved organics in the droplet. The presence of inorganic salts may potentially modify the effect of dissolved organic compounds, as the surface tension of electrolytic solutions increases with the molality of inorganic salts. However, the electrolyte concentrations in recently activated CCN are typically not large enough to induce a significant change in surface tension (e.g., Pruppacher and Klett 1997). This argument is supported by measurements of CCN activity for laboratory-generated particles; no corrections in surface tension are needed for describing the properties of pure-salt CCN. Nevertheless, if inorganic salts appreciably increase surface tension, that would be reflected in the Facchini et al. (1999) measurements applied in our study, as their measurements did contain inorganics in their cloud water samples.

Substitution of Eq. (3) into the expression for the curvature coefficient, A, leads to

$$A = \frac{2M_w}{RT\rho_w}[\sigma_s^* - A_1 T \ln(1 + A_2 C)], \tag{4}$$

where $C = v_c n_o/V_{drop}$, v_c is the number of moles of carbon in one mole of the soluble organic compound, n_o is the number of moles of the dissolved organic species and $n_o = 4\pi\varepsilon_o \rho_{ap} a_d^3/(3M_o)$, V_{drop} is the volume of the droplet, and $V_{drop} = 4\pi r^3/3$. Substituting the expression for C into Eq. (4) gives

$$A = A^* - A_4 T \ln\left(1 + \frac{A_3 a_d^3}{r^3}\right), \qquad (5)$$

where $A^* = 2M_w\sigma_s^*/(RT\rho_w)$, $A_3 = \varepsilon_o v_c \rho_{ap} A_2 / M_o$, and $A_4 = 2M_w A_1/(R\rho_w)$. Note that as the droplet grows, the dissolved organic concentration decreases and the droplet surface tension approaches that of pure water. Substituting Eq. (5) into Eq. (1) gives the extended Köhler expression, which includes surface tension changes due to dissolved organic components, as well as insoluble components:

$$s = \frac{A^*}{r} - \frac{A_4}{r}\ln\left(1 + \frac{A_3 a_d^3}{r^3}\right) - \frac{B a_d^3}{r^3 - b_1 a_d^3}. \qquad (6)$$

Compared to an aerosol particle containing a certain amount of inorganic and insoluble species, an increase in the organic mass fraction can (i) decrease the supersaturation by decreasing the surface tension [which is reflected in the second term in Eq. (6)]; (ii) change the supersaturation by changing the moles of dissolved species in the aerosol [reflected by changes in the B coefficient of the third term in Eq. (6)]; depending on the relative proportions of organic and inorganic species, increasing the organic mass fraction can either increase or decrease the supersaturation; and (iii) increase the supersaturation by decreasing the b_1 term in the denominator of the third term in Eq. (6), assuming that the organic mass fraction increases at the expense of the insoluble mass fraction. This influence is important for diameters exceeding the critical diameter.

b. Simplifications of the full Köhler expression

The critical properties for the droplet are determined at the maximum of Eq. (6):

$$\frac{ds}{dr} = 0 = -\frac{A^*}{r_c^2} + \frac{A_4}{r_c^2}\ln\left(1 + \frac{A_3 a_d^3}{r_c^3}\right)$$
$$+ \frac{3A_3 A_4 a_d^3}{\left(1 + \frac{A_3 a_d^3}{r_c^3}\right) r_c^5} + \frac{3 B a_d^3 r_c^2}{(r_c^3 - b_1 a_d^3)^2}. \qquad (7)$$

Certain approximations can be made to obtain an explicit expression for the critical droplet radius. We approximate the Köhler curve with one of constant surface tension, and the same critical diameter and critical supersaturation. The constant surface tension, σ_s^*, instead of being that of pure water, is now assigned a value computed from the organic concentration at the critical radius. Classical Köhler theory is used to calculate the critical radius, assuming $\sigma_s = \sigma_s^*$, $r_c^* = (3 B a_d^3/A^*)^{1/2}$ (Seinfeld and Pandis 1998). Substitution into Eq. (6) leads to a simplified Köhler equation:

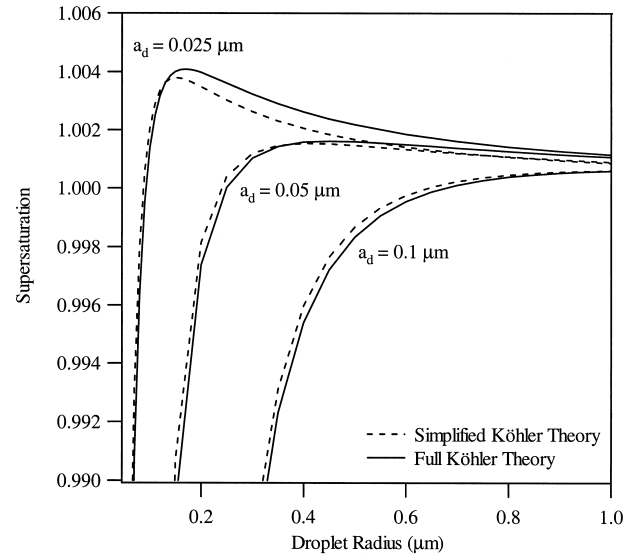$$s = \frac{A_{5d}}{r} - \frac{B a_d^3}{r^3}, \qquad (8)$$

FIG. 1. Köhler curves for the simplified Köhler theory and full Köhler theory for three different dry radii (a_d) for the aerosol characteristics in Table 1. The inorganic compound is assumed to be ammonium sulfate. The soluble organic component is assumed to have the properties of a mixture of 18% levoglucosan, 41% succinic acid, and 41% fulvic acid, by mass (Nenes et al. 2002). The insoluble component is assumed to have the properties of typical mineral dust.

where $A_{5d} = A^* - A_4 \ln[1 + (A_3 a_d^3/r_c^{*3})]$. The critical radius is now explicitly given by

$$r_c = \left(\frac{3 B a_d^3}{A_{5d}}\right)^{1/2}. \qquad (9)$$

Equation (8), though a simplification, is self consistent. When $\varepsilon_o \to 0$, the surface tension goes to that of water ($\sigma_s \to \sigma_s^*$) and $A_{5d} \to A$, so the expression reduces to classical Köhler theory. Furthermore, the simplification does not introduce significant error, as is shown by Fig. 1.

The dry radii examined are 0.025, 0.05, and 0.1 μm, typical of relevant CCN sizes. Table 1 summarizes the aerosol properties used, which correspond to a mixture of inorganic and organic compounds and mineral dust. The error in the critical supersaturation (between the simplified and full treatments) is below 10% for critical supersaturations less than 1% and never exceeds 15%, even for supersaturations as high as 3.5%. Since atmospheric supersaturations are typically below 1%, the error incurred in the critical supersaturation by using Eqs. (8) and (9) for atmospheric conditions is expected to be less than 10%.

c. Single-mode parameterization modification

The fraction of particles that activate to droplets is given by Abdul-Razzak et al. (1998) and Abdul-Razzak and Ghan (2000) as

TABLE 1. Aerosol characteristics used to analyze the accuracy of the modified Köhler expression.

Aerosol characteristics	Symbol	Value
Organic mixture properties	ε_o	0.1
	ρ_o	1.55 g cm^{-3}
	M_o	194.33 g mol^{-1}
	v_o	2.79
	v_c	8.94
(NH$_4$)$_2$SO$_4$ properties	ε_s	0.5
	ρ_s	1.76 g cm^{-3}
	M_S	132 g mol^{-1}
	v_s	3
Insoluble compound properties	ε_{ins}	0.4
	ρ_{ins}	2 g cm^{-3}
Aerosol size distribution properties	N_{ap}	200 cm^{-3}
	σ	2.5
	a_m	0.01 μm
Other constants	T	273 K
	A_1	1.87×10^{-7} N cm^{-1} K^{-1}
	A_2	6.28×10^5 cm^3 mol^{-1}
	σ_s^*	7.28×10^{-4} N cm^{-1}

$$\frac{N}{N_{\text{ap}}} = \frac{1}{2}[1 - \text{erf}(u)], \tag{10}$$

where $u = \ln(a_c/a_m)/[\sqrt{2}\ln(\sigma)]$, N is the droplet number concentration, N_{ap} is the total aerosol number concentration, a_c is the dry radius of the smallest activated particle, a_m is the mean dry radius of the aerosol size distribution, and σ is the geometric standard deviation of the aerosol size distribution.

To account for surface tension changes due to the dissolved organics, the radii a_c and a_m are computed from the simplified Köhler theory through their corresponding critical supersaturations. The maximum supersaturation, s_{max}, corresponds to the critical supersaturation of the smallest activated particle:

$$s_{\text{max}} = \frac{2}{\sqrt{B}}\left(\frac{A_{5c}}{3a_c}\right)^{3/2}, \tag{11}$$

where $A_{5c} = A^* - A_4 \ln[1 + (A_3a_c^3/r_c^{*3})]$. The critical supersaturation, s_m, of a particle with dry radius equal to the geometric mean radius of the aerosol size distribution is given by

$$s_m = \frac{2}{\sqrt{B}}\left(\frac{A_{5m}}{3a_m}\right)^{3/2}, \tag{12}$$

where $A_{5m} = A^* - A_4 \ln[1 + (A_3a_m^3/r_c^{*3})]$. Equations (11) and (12) must be solved for a_c and a_m and substituted into the expression for u. The dependencies of A_{5m} and A_{5c} on a_m and a_c, respectively, preclude explicit expressions; however, if $r_c^* \ll A_3a_d$, then $A_3a_d^3/r_c^{*3} \gg 1$, $\ln[1 + (A_3a_d^3/r_c^{*3})] \approx \ln(A_3a_d^3/r_c^{*3})$, and

$$A_{5i} = A^* - A_4 \ln\left(\frac{A_3a_i^3}{r_c^{*3}}\right) \qquad i = d, m, c. \tag{13}$$

d. Analysis of A_{5d}, A_{5m}, and A_{5c} parameter simplifications

The errors arising from the assumptions used in the development of Eq. (13) increase with increases in a_d and decreases in a_c and a_m. It can be shown that the absolute error in the A_{5d} parameter is less than 5% for a_d less than 0.1 μm. For the A_{5m} and A_{5c} parameters, the absolute errors are less than 40% for a_d, a_m, and a_c less than 0.1 μm. The accuracy with which the EAGR parameterization is able to assess the sensitivity of the droplet number concentration to chemical and microphysical parameters should be sufficient for this study, although for very low updrafts and very large particle sizes, the error can be large (Nenes and Seinfeld 2003). The former situations are infrequent, while the latter case would activate easily, so neither is expected to give a gross error. For most cases, the droplet number concentration is most sensitive to particles that activate at supersaturations close to the maximum supersaturation of the parcel. The radii of such particles are usually in the range of 0.05–0.15 μm (Nenes et al. 2001). The performance of the EAGR parameterization will be evaluated subsequently by comparing its predictions to those of a full, numerical parcel model.

Equation (13) is expanded to

$$A_{5i} = A^* - A_4 \ln\left(\frac{A_3a_i^3}{r_c^{*3}}\right) = A^* - A_4 \ln\left(\frac{A_3a_i^3}{r_c^{*3}}\frac{\lambda}{\lambda}\right)$$

$$= A^* - A_4 \ln\left(\frac{A_3}{\lambda r_c^3}\right) - A_4 \ln(\lambda a_i^3)$$

$$= A' - 3A_4 \ln(\lambda^{1/3}a_i) = A' - A_6 \ln(a_i), \tag{14}$$

where $A' = A^* - A_4 \ln(A_3/r_c^{*3})$, $A_6 = 3A_4$, and $\lambda = 1$ (length)$^{-3}$. Substituting Eq. (14) into Eqs. (12) and (11), we obtain

$$s_{\text{max}} = \frac{2}{\sqrt{B}}\left[\frac{A' - A_6 \ln(a_c)}{3a_c}\right]^{3/2} \quad \text{and} \tag{15a}$$

$$s_m = \frac{2}{\sqrt{B}}\left[\frac{A' - A_6 \ln(a_m)}{3a_m}\right]^{3/2}. \tag{15b}$$

To obtain explicit expressions for a_c and a_m, one more approximation to Eqs. (15a) and (15b) is needed, which is to substitute the logarithmic terms with average values of a_c and a_m that are relevant for the atmosphere. The range of values for a_m is taken from Whitby (1978), and the limits for a_c are set at twice the limits of a_m:

$$\ln(a_c) \approx \overline{\ln(a_c)} = \int_{1\times10^{-7}\text{cm}}^{1\times10^{-6}\text{cm}} \ln(a_c)\, da_c = -14.6 \tag{16a}$$

and

$$\ln(a_m) \approx \overline{\ln(a_m)} = \int_{2\times10^{-7}\text{cm}}^{2\times10^{-6}\text{cm}} \ln(a_m)\, da_m = -13.9. \tag{16b}$$

TABLE 2. Equations for physical parameters G, α, and γ (Pruppacher and Klett 1997).

Equation	Symbol definitions
$\alpha = \dfrac{gM_wL}{C_{pa}RT^2} - \dfrac{gM_{air}}{RT}$	α = radius-independent coefficient g = acceleration due to gravity L = latent heat of vaporization of water C_{pa} = specific heat of dry air at constant pressure M_{air} = molar mass of air
$\gamma = \dfrac{RT}{p_sM_w} + \dfrac{M_wL^2}{C_{pa}pM_{air}T}$	γ = radius-independent coefficient p_s = saturation vapor pressure p = pressure
$G = \dfrac{1}{\dfrac{\rho_wRT}{p_sD_VM_w} + \dfrac{L\rho_w}{K_aT}\left(\dfrac{LM_w}{RT} - 1\right)}$	G = growth coefficient D_V = diffusivity of water in air K_a = thermal conductivity of air

The total error incurred by the assumptions and approximations that have been made throughout this derivation will be analyzed in section 2f by comparing the predictions of the approximate model to those of a detailed parcel model. The numerical values used in Eqs. (16a) and (16b) are not optimized and can be further adjusted based on datasets other than those of Whitby (1978).

e. The modified parameterization (single mode)

Solving Eqs. (15a) and (15b) for a_c and a_m, with the aforementioned approximations, results in the following expressions:

$$a_c = \frac{A' - A_6\,\overline{\ln(a_c)}}{3}\left(\frac{2}{\sqrt{B}s_{max}}\right)^{2/3} \quad \text{and} \quad (17a)$$

$$a_m = \frac{A' - A_6\,\overline{\ln(a_m)}}{3}\left(\frac{2}{\sqrt{B}s_m}\right)^{2/3}. \quad (17b)$$

Substituting Eqs. (17a) and (17b) into the expression for u leads to the following expression:

$$u = \frac{\ln[k_c(s_m/s_{max})^{2/3}]}{\sqrt{2}\,\ln(\sigma)}, \quad (18)$$

where

$$k_c = \frac{A' - A_6\,\overline{\ln(a_c)}}{A' - A_6\,\overline{\ln(a_m)}}. \quad (19)$$

The error function of the u parameter [erf(u)] represents the fraction of the total aerosol number concentration that remains as interstitial aerosol after activation has taken place.

The maximum parcel supersaturation is obtained by Abdul-Razzak et al. (1998) by using the functions $f_1(\ln\sigma)$ and $f_2(\ln\sigma)$, which are used to fit the ratio of
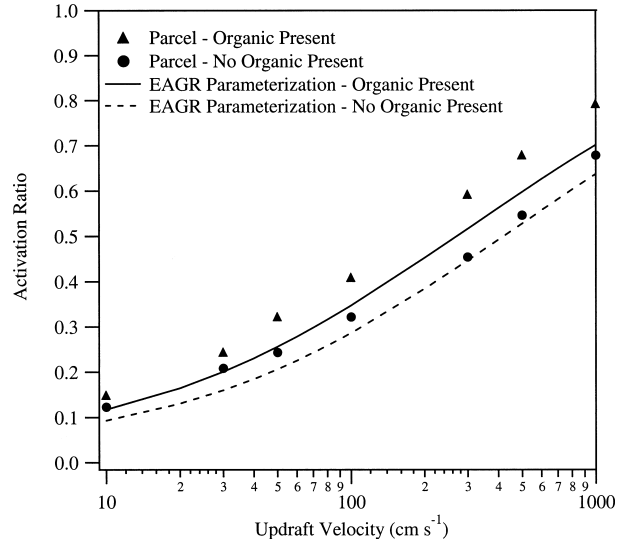

FIG. 2. Activation ratio as a function of updraft velocity for the full numerical parcel model and the EAGR parameterization, in the presence and absence of dissolved organic material. The aerosol is 10% organic and 90% $(NH_4)_2SO_4$ when organics are present. Properties of the organic material and ammonium sulfate and the aerosol size distribution are given in Table 1.

s_m and s_{max} to a numerical solution of the governing equations:

$$\left(\frac{s_m}{s_{max}}\right)^2 = f_1(\ln\sigma)\left(\frac{\zeta}{\eta}\right)^{3/2} + f_2(\ln\sigma)\left(\frac{s_m^2}{\eta + 3\zeta}\right)^{3/4}, \quad (20)$$

where $f_1(\ln\sigma) = 0.5\,\exp[2.5\,\ln^2(\sigma)]$, $f_2(\ln\sigma) = 1 + 0.25\,\ln(\sigma)$, $\zeta = 2/3(\alpha W/G)^{1/2}A_{5c}$, $\eta = [1/(2\pi\rho_w\gamma N_{ap})](\alpha W/G)^{3/2}$, and W is the updraft velocity. All other parameters are defined in Table 2. These expressions for $f_1(\ln\sigma)$ and $f_2(\ln\sigma)$ are the corrected expressions given in Abdul-Razzak and Ghan (2000) for a multimodal aerosol. Note also that the expression for ζ differs from the original expression given by Abdul-Razzak et al. (1998), in that the A parameter is replaced with the A_{5c} parameter.

Surface tension changes of the growing droplet introduce two new quantities: the k_c parameter in the u function [Eq. (18)] and the A_{5c} parameter in the ζ parameter. The k_c parameter accounts for the differences in the radii, a_m and a_c. The A_{5c} parameter takes into account the surface tension changes. When surface tension effects become negligible, $k_c \to 1$, and the original parameterization of Abdul-Razzak et al. (1998) is obtained.

f. Comparison to a numerical parcel model

The EAGR parameterization is compared to an adiabatic parcel model with explicit microphysics to evaluate its ability to represent particle activation (Nenes et al. 2002a). Figure 2 shows the activation ratio as a function of updraft velocity as computed with the parcel model and with the surface tension parameterization.

TABLE 3. Multimodal surface tension parameterization.

Equations

$$N = \sum_{i=1}^{I} \frac{N_{\mathrm{api}}}{2}[1 - \mathrm{erf}(u_i)]*$$

$$B_i = \left(\frac{M_w \rho_{\mathrm{api}}}{\rho_w}\right)\left(\frac{\varepsilon_{\mathrm{si}} v_{\mathrm{si}}}{M_{\mathrm{si}}} + \frac{\varepsilon_{\mathrm{oi}} v_{\mathrm{oi}}}{M_{\mathrm{oi}}}\right)$$

$$s_{\max} = \frac{1}{\left\{\sum_{i=1}^{I} \frac{1}{s_{\mathrm{mi}}^2}\left[f_{1i}(\sigma_i)\left(\frac{\zeta_i}{\eta_i}\right)^{3/2} + f_{2i}(\sigma_i)\left(\frac{s_{\mathrm{mi}}^2}{\eta_i + 3\zeta_i}\right)^{3/4}\right]\right\}^{1/2}}*$$

$$f_1(\sigma_i) = 0.5 \exp[2.5 \ln^2(\sigma_i)]*$$

$$f_2(\sigma_i) = 1 + 0.25 \ln(\sigma_i)*$$

$$\eta_i = \frac{1}{2\pi\rho_w \gamma N_{\mathrm{api}}}\left(\frac{\alpha W}{G}\right)^{3/2}*$$

$$A_i' = A* - A_4 \ln\left(\frac{A_{3i}}{r_{\mathrm{ci}}^{*3}}\right)$$

$$r_{\mathrm{ci}}^* = \left(\frac{3B_i a_{\mathrm{mi}}^3}{A*}\right)^{1/2}$$

$$A_{3i} = \frac{\varepsilon_{\mathrm{oi}} v_{\mathrm{ci}} \rho_{\mathrm{api}} A_2}{M_{\mathrm{oi}}}$$

* From Abdul-Razzak and Ghan (2000).

The activation ratio calculated using the EAGR parameterization differs from that calculated using the parcel model. Part of this discrepancy is inherent in the original Abdul-Razzak et al. (1998) parameterization (as can be seen by comparing the predictions of droplet number concentration in the absence of surface tension effects). Nevertheless, the EAGR parameterization reasonably captures the relative change in maximum supersaturation and droplet number concentration when a soluble organic compound is introduced into the aerosol. The presence of surface tension effects decreases the maximum supersaturation by 10% in both the EAGR parameterization and the parcel model. Thus, derivatives of the EAGR expression for the number of particles activated should give physically realistic sensitivities to variations of key parameters, and especially relative sensitivities.

g. Extension of EAGR parameterization to multimodal aerosol populations

The multimode lognormal aerosol size distribution is given by

$$n(\ln a_d) = \sum_{i=1}^{I} \frac{N_{\mathrm{api}}}{\sqrt{(2\pi)}\ln(\sigma_i)} \exp\left[-\frac{\ln^2(a_d/a_{\mathrm{mi}})}{2\ln^2(\sigma_i)}\right], \quad (21)$$

where the subscript i indicates a quantity that is specific to aerosol population mode i.

The generalized parameterization for a multimodal aerosol population consists of the equations in Table 3. Some of the parameter definitions differ from those in Abdul-Razzak and Ghan (2000) because the Köhler curvature coefficient, A, has been replaced with the mod-

ified coefficients, $A_{5\mathrm{mi}}$ and $A_{5\mathrm{ci}}$, in the ζ parameter and s_m:

$$s_{\mathrm{mi}} = \frac{2}{\sqrt{B_i}}\left(\frac{A_{5\mathrm{mi}}}{3a_{\mathrm{mi}}}\right)^{3/2} \quad \text{and}$$

$$\zeta_i = \frac{2}{3}\left(\frac{\alpha W}{G}\right)^{1/2} A_{5\mathrm{ci}}, \quad (22)$$

where $A_{5ji} = A_i' - A_6 \ln(\overline{a_j})$. In the expression for A_{5ji}, a_j represents the geometric mean radius ($j = m$) or the radius of the smallest activated aerosol particle ($j = c$). A new parameter, $k_{\mathrm{ci}} = A_{5\mathrm{ci}}/A_{5\mathrm{mi}}$, is introduced in the u_i parameter to account for the differences in the a_c and a_m:

$$u_i = \frac{\ln[k_{\mathrm{ci}}(s_{\mathrm{mi}}/s_{\max})^{2/3}]}{\sqrt{2}\,\ln(\sigma_i)}. \quad (23)$$

3. Sensitivity analysis

Using the EAGR parameterization, the sensitivity of the activated droplet number concentration, N, with respect to any parameter χ, where χ denotes ε_o, σ, N_{ap}, or a_m, is given by

$$dN/d\chi_j = (\partial N/\partial \chi_j) + (\partial N/\partial u_j)(\partial u_j/\partial \chi_j), \quad (24)$$

where the subscript j indicates that the parameter can be specific to a single mode of a multimodal aerosol size distribution (e.g., the geometric mean radius of the coarse mode) and

$$\frac{\partial N}{\partial u_j} = -\sum_{i=1}^{I}\left(\frac{N_{\mathrm{api}}}{\sqrt{\pi}}\right)\exp(-u_i^2). \quad (25)$$

Equation (25) can be evaluated for a unimodal aerosol population for $i, j = 1$. Here, $\partial N/\partial \chi_j = 0$ for all χ_j, other than the total aerosol number concentration, N_{apj}:

$$\partial N/\partial N_{\mathrm{apj}} = (1/2)[1 - \mathrm{erf}(u_j)]. \quad (26)$$

Equation (24) for $\chi_j = N_{\mathrm{ap}}$ is exactly the Twomey effect, because it describes the sensitivity of N to N_{ap}. The sensitivities of N to all other aerosol properties, except for size distribution characteristics, are considered to represent the chemical effects, and the sensitivity of N to W describes the dynamical effects.

Expressions for the sensitivity of N with respect to the updraft velocity (W), N_{apj}, organic mass fraction (ε_o), and geometric standard deviation (σ) and geometric mean radius (a_m) of the aerosol size distribution are given in Table 4 for unimodal and multimodal aerosols. Although the latter sensitivities (e.g., with respect to σ, a_m) are not from chemical effects on aerosols, we have included them in this study for completeness. The unimodal derivatives can be obtained from the multimodal derivatives by letting $i, j = 1$ and replacing the multimodal $f_{1i}(\sigma_i)$ and $f_{2i}(\sigma_i)$ with the unimodal $f_1(\ln\sigma)$ and $f_2(\ln\sigma)$, respectively, except in the σ case.

TABLE 4. Derivatives of the droplet number concentration with respect to various χ_j for a multimodal aerosol population.*

χ_j	$\dfrac{\partial u_i}{\partial \chi_j}$	$\dfrac{\partial s_{mj}}{\partial \chi_j}$	$\dfrac{\partial s_{max}}{\partial \chi_j}$
W	$-\dfrac{\sqrt{2}}{3\ln(\sigma_i)s_{max}}\dfrac{\partial s_{max}}{\partial W}$	0	$\sum_{i=1}^{I}\dfrac{3}{2Ws_{mi}^2}\left[-f_{1i}(\sigma_i)\left(\dfrac{\zeta_i}{\eta_i}\right)^{3/2} + \dfrac{3f_{2i}(\sigma_i)s_{mi}^{3/2}}{4(\eta_i + 3\zeta_i)^{7/4}}(\eta_i + \zeta_i)\right]\Bigg/\left\{2\left[\sum_{i=1}^{I}\dfrac{1}{s_{mi}^2}\left[f_{1i}(\sigma_i)\left(\dfrac{\zeta_i}{\eta_i}\right)^{3/2} + f_{2i}(\sigma_i)\left(\dfrac{s_{mi}^2}{\eta_i + 3\zeta_i}\right)^{3/4}\right]\right]^{3/2}\right\}$
N_{apj}	$-\dfrac{\sqrt{2}}{3\ln(\sigma_i)s_{max}}\dfrac{\partial s_{max}}{\partial N_{apj}}$	0	$\dfrac{3}{2s_{mj}^2 N_{apj}}\left[f_{1j}(\sigma_j)\left(\dfrac{\zeta_j}{\eta_j}\right)^{3/2} - \dfrac{f_{2j}(\sigma_j)s_{mj}^{3/2}\eta_j}{2(\eta_j + 3\zeta_j)^{7/4}}\right]\Bigg/\left\{2\left[\sum_{i=1}^{I}\dfrac{1}{s_{mi}^2}\left[f_{1i}(\sigma_i)\left(\dfrac{\zeta_i}{\eta_i}\right)^{3/2} + f_{2i}(\sigma_i)\left(\dfrac{s_{mi}^2}{\eta_i + 3\zeta_i}\right)^{3/4}\right]\right]^{3/2}\right\}$
ε_{oj}**	$\dfrac{A_4}{\sqrt{2}\ln(\sigma_j)}\left(\dfrac{1}{A_{5cj}} - \dfrac{1}{A_{5mj}}\right)\left[\dfrac{3M_w v_{oj}\rho_{apj}}{2M_{oj}\rho_w B_j} + \dfrac{\rho_{apj}}{2}\left(\dfrac{1}{\rho_{insj}} - \dfrac{1}{\rho_{oj}}\right) - \dfrac{1}{\varepsilon_{oj}}\right]$ $+ \dfrac{\sqrt{2}}{3\ln(\sigma_j)}\left(\dfrac{1}{s_{mj}}\dfrac{\partial s_{mj}}{\partial \varepsilon_{oj}} - \dfrac{1}{s_{max}}\dfrac{\partial s_{max}}{\partial \varepsilon_o}\right)$ $(i = j)$ $-\dfrac{\sqrt{2}}{3\ln(\sigma_j)s_{max}}\dfrac{\partial s_{max}}{\partial \varepsilon_o}$ $(i \neq j)$	$\dfrac{s_{mj}M_w v_{oj}\rho_{apj}}{2B_j M_{oj}\rho_w}\left(\dfrac{9A_4}{2A_{5mj}} - 1\right)$ $+ \dfrac{s_{mj}\rho_{apj}}{2}\left(\dfrac{1}{\rho_{insj}} - \dfrac{1}{\rho_{oj}}\right)\left(\dfrac{3A_4}{2A_{5mj}} - 1\right)$	$-\dfrac{3\zeta_j A_4}{2A_{5cj}s_{mj}^{1/2}}\left[\dfrac{2f_{1j}(\sigma_j)}{s_{mj}^{3/2}}\left(\dfrac{\zeta_j}{\eta_j}\right)^{3/2} + \dfrac{f_{2j}(\sigma_j)}{2(\eta_j + 3\zeta_j)^{3/4}}\right]\dfrac{1}{s_{mj}^2}\dfrac{\partial s_{mj}}{\partial \varepsilon_{oj}}\Bigg/\left\{2\left[\sum_{i=1}^{I}\dfrac{1}{s_{mi}^2}\left[f_{1i}(\sigma_i)\left(\dfrac{\zeta_i}{\eta_i}\right)^{3/2} + f_{2i}(\sigma_i)\left(\dfrac{s_{mi}^2}{\eta_i + 3\zeta_i}\right)^{3/4}\right]\right]^{3/2}\right\}$
σ_j (multimodal)	$-\dfrac{1}{\sqrt{2}\sigma_j \ln^2(\sigma_j)}\ln\left[k_{cj}\left(\dfrac{s_{mj}}{s_{max}}\right)^{2/3}\right] - \dfrac{\sqrt{2}}{3\ln(\sigma_j)s_{max}}\dfrac{\partial s_{max}}{\partial \sigma_j}$ $(i = j)$ $-\dfrac{\sqrt{2}}{3\ln(\sigma_j)s_{max}}\dfrac{\partial s_{max}}{\partial \sigma_j}$ $(i \neq j)$	0	$\dfrac{1}{\sigma_j s_{mj}^{1/2}}\left[\dfrac{5\ln(\sigma_j)f_{1j}(\sigma_j)}{s_{mj}^{3/2}}\left(\dfrac{\zeta_j}{\eta_j}\right)^{3/2} - \dfrac{0.25}{(\eta_j + 3\zeta_j)^{3/4}}\right]\Bigg/\left\{2\left[\sum_{i=1}^{I}\dfrac{1}{s_{mi}^2}\left[f_{1i}(\sigma_i)\left(\dfrac{\zeta_i}{\eta_i}\right)^{3/2} + f_{2i}(\sigma_i)\left(\dfrac{s_{mi}^2}{\eta_i + 3\zeta_i}\right)^{3/4}\right]\right]^{3/2}\right\}$
σ (unimodal)	$-\dfrac{1}{\sqrt{2}\sigma \ln^2(\sigma)}\ln\left[k_c\left(\dfrac{s_m}{s_{max}}\right)^{2/3}\right] - \dfrac{\sqrt{2}}{3\ln(\sigma)s_{max}}\dfrac{\partial s_{max}}{\partial \sigma}$	0	$\dfrac{s_m}{\sigma}\left[4.5\ln(\sigma)f_1(\ln\sigma)\left(\dfrac{\zeta}{\eta}\right)^{3/2} + 0.25\left(\dfrac{s_m^2}{\eta + 3\zeta}\right)^{3/4}\right]\Bigg/\left\{2\left[f_1(\ln\sigma)\left(\dfrac{\zeta}{\eta}\right)^{3/2} + f_2(\ln\sigma)\left(\dfrac{s_m^2}{\eta + 3\zeta}\right)^{3/4}\right]^{3/2}\right\}$
a_{mj}	$-\dfrac{9A_{s4}}{2\sqrt{2}a_{mj}\ln(\sigma_j)}\left(\dfrac{1}{A_{5cj}} - \dfrac{1}{A_{5mj}}\right)$ $+ \dfrac{\sqrt{2}}{3\ln(\sigma_j)}\left(\dfrac{1}{s_{mj}}\dfrac{\partial s_{mj}}{\partial a_{mj}} - \dfrac{1}{s_{max}}\dfrac{\partial s_{max}}{\partial a_{mj}}\right)$ $(i = j)$ $-\dfrac{\sqrt{2}}{3\ln(\sigma_j)s_{max}}\dfrac{\partial s_{max}}{\partial a_{mj}}$ $(i \neq j)$	$\dfrac{3s_{mj}}{2a_{mj}}\left(\dfrac{9A_4}{2A_{5mj}} - 1\right)$	$-\dfrac{27A_4\zeta_j}{4A_{5cj}a_{mj}}\left[\dfrac{f_{1j}(\sigma_j)}{\eta_j s_{mj}^{3/2}}\left(\dfrac{\zeta_j}{\eta_j}\right)^{1/2} + \dfrac{f_{2j}(\sigma_j)}{2s_{mj}^{3/2}(\eta_j + 3\zeta_j)^{3/4}} - \dfrac{3f_{2j}(\sigma_j)}{2(\eta_j + 3\zeta_j)^{7/4}}\right]\dfrac{\partial s_{mj}}{\partial a_{mj}}\Bigg/\left\{2\left[\sum_{i=1}^{I}\dfrac{1}{s_{mi}^2}\left[f_{1i}(\sigma_i)\left(\dfrac{\zeta_i}{\eta_i}\right)^{3/2} + f_{2i}(\sigma_i)\left(\dfrac{s_{mi}^2}{\eta_i + 3\zeta_i}\right)^{3/4}\right]\right]^{3/2}\right\}$

* See Table 3 and text for equations for ζ_i, η_i, $f_{1i}(\sigma_i)$, $f_{2i}(\sigma_i)$, A_{Sci}, A_{5mi}, s_{mi}, s_{max}, B_i, ρ_{api}, and A_4.

** Here, ε_{sj} is held constant.

TABLE 5. Cases examined in sensitivity analysis.

	Case 1	Case 2	Case 3	Case 4	Case 5	Case 6	Case 7
χ in $\phi(\chi)$	ε_o	ε_o	ε_o	ε_o	a_m	a_m	a_m
Surface tension effects	Present	Present	Present	Present	Absent	Absent	Absent
Aerosol size distribution	Marine	Marine	Continental	Continental	Continental	Marine	Continental
Unimodal or trimodal	Trimodal	Trimodal	Trimodal	Trimodal	Unimodal	Trimodal	Trimodal
Insoluble mass fraction	0	0.5	0	0.5	0	0	0

From these expressions, we note that $\partial N/\partial W > 0$ because $\partial u_j/\partial W \geq 0$. For the other variables, $\partial N/\partial \chi$ can be either positive or negative, and the sign will determine the relative importance of the chemical effects. This is an important difference between chemical and dynamical effects, as an increase in χ, which corresponds to a region of increased biomass burning or biogenic emissions, can enhance or decrease the sensitivity of N with respect to W. Note that this assumes that $\chi_j = N_{ap}$, σ, and ε_o (or ε_i) usually increase for increasingly polluted aerosols.

To examine the sensitivity of droplet number concentration to chemical effects relative to the sensitivity to dynamical effects (updraft velocity), we scale the sensitivities to the same order by adopting the nondimensional form:

$$\phi(\chi) = \frac{\chi}{W}\frac{\partial N/\partial \chi}{\partial N/\partial W}, \qquad (27)$$
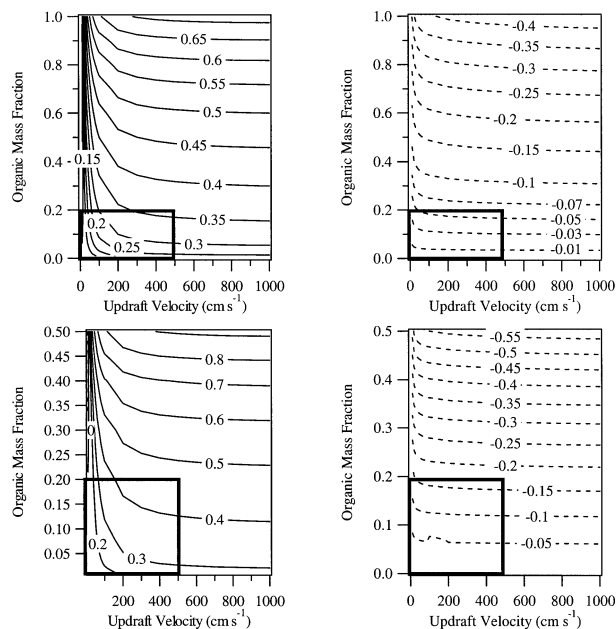

FIG. 3. Sensitivity ratio $\phi(\varepsilon_o)$ for a marine aerosol size distribution with (left) surface tension effects and (right) without surface tension effects. The aerosol consists of $(NH_4)_2SO_4$ and dissolved organics with (top) no insoluble species present and (bottom) 50% insoluble species. The inner rectangles represent typical organic mass fraction and updraft velocity ranges for marine, stratocumulus conditions. Solid lines represent positive $\phi(\varepsilon_o)$ values; dashed lines represent negative $\phi(\varepsilon_o)$ values.

where the derivatives are evaluated at a nominal set of parameter values, evaluated from Eq. (24). When $|\phi(\chi)| \sim 1$, N is equally sensitive to changes in W and χ. When $|\phi(\chi)| \gg 1$, χ can dominate over changes in W; while when $|\phi(\chi)| \ll 1$, N is relatively insensitive to χ. Positive values of $\phi(\chi)$ indicate that increasing χ and W both change N in the same direction (either both increase N or both decrease N). Negative values of $\phi(\chi)$ indicate that χ and W change N in opposite directions.

The sensitivity ratio, $\phi(\chi)$, is evaluated for the seven aerosol types given in Table 5. The aerosol size distribution characteristics are obtained from Whitby (1978). The parameters chosen for investigation are the soluble organic mass fraction (constant for all modes) and the geometric mean radius (a_m). The presence of insoluble material in the dry aerosol is also considered. The soluble inorganic portion of the aerosol is assumed to be ammonium sulfate. For the trimodal aerosol, the accumulation mode geometric mean radius is chosen as the parameter of interest because it generally has the greatest influence on the droplet number concentration. Surface tension effects are not included in the mean radius sensitivity cases. The sensitivity ratio in the absence of surface tension effects leads to effects of smaller magnitude than with surface tension effects included in the mean radius cases.

Figure 3 shows $\phi(\varepsilon_o)$ for marine aerosol (left panels) with and (right panels) without surface tension effects; we present results for (top panels) in the absence and (bottom panels) presence of insoluble species. The rectangles represent the range of updraft velocities and organic mass fractions found in the atmosphere for stratocumulus clouds under marine conditions (Seinfeld and Pandis 1998). The general trend is that $\phi(\varepsilon_o)$, and thus the relative influence of the chemical effect, increases with increasing ε_o and W. This means that an increase in surface active organic component would tend to further enhance droplet formation compared to an aerosol composed of pure salt. This is clear when comparing to $\phi(\varepsilon_o)$ without surface tension effects; in this case, $\phi(\varepsilon_o)$ is negative because the dissolved moles of salt decrease with increasing organic fraction. Surface tension effects seem to compensate for the decreased hygroscopicity of the organic fraction, and increase the sensitivity of droplet number to variations in the updraft spectrum. The latter can be seen in Fig. 3, where the lack of surfactant behavior yields an almost constant $\phi(\varepsilon_o)$ for all updraft velocities. Once a surfactant is

placed in the CCN, $\phi(\varepsilon_o)$ is variable for a large range of updraft velocities, certainly under the range expected for marine stratocumulus. In the absence of insoluble species, $\phi(\varepsilon_o)$ ranges from 0.1 to 0.35 for typical marine conditions; with an insoluble mass fraction of 0.5, the sensitivity ratio ranges from 0 to 0.45. These values are consistent with the simulations of a detailed, numerical parcel model (Nenes et al. 2002a). Although $\phi(\varepsilon_o)$ (in the presence of surfactant species) is positive for most cases, negative values of $\phi(\varepsilon_o)$ occur in the lower panel of Fig. 3 at very low W (<10 cm s^{-1}) and high ε_o (0.20–0.5). This means that an increase in ε_o would lead to a decrease in N because $\partial N/\partial W > 0$. Also, $\partial N/\partial \varepsilon_o < 0$ because, relative to the case with no soluble organic present [i.e., $\phi(0)$], more CCN activate earlier in the cloud updraft and deplete water vapor from the gas phase. As a result, the maximum supersaturation drops and, with it, the total number of activated CCN. Such dynamical readjustments are most effective under polluted conditions, such as the competition between sea salt and sulfate for CCN (Ghan et al. 1998) and black carbon effects on cloud microphysics (Nenes et al. 2002b). However, for larger values of W, increases in ε_o lead to increases in the sensitivity. Although interesting, this effect occurs at values of ε_o and W that are not typically found in the marine atmosphere. Therefore, for most marine aerosols, $\phi(\varepsilon_o) > 0$. Given that $\phi(\varepsilon_o)$ has a magnitude between 0.1 and 0.5 under marine conditions, one concludes that surface tension effects can exhibit an important effect on activated droplet number concentration (when present). For a given ε_o, $\phi(\varepsilon_o)$ increases with updraft velocity, because the maximum supersaturation increases, and, thus, the potential for CCN activation is greater (this effect is not seen when the surface tension effect is excluded). However, as smaller nuclei activate, decreases in surface tension are less effective in facilitating activation, because the concentration of soluble organics at the critical diameter drops as the particle dry diameter decreases [see Eqs. (8) and (9)]. The latter effect leads to an "asymptotic" limit in $\phi(\varepsilon_o)$, which is generally reached, for the current set of parameters, at an updraft velocity of 5 m s^{-1}. Mathematically, this limit can be derived by $\partial^2 N/\partial \varepsilon_o^2 = \partial^2 N/\partial W^2$. At low updraft velocities (in the presence of surfactants), $\phi(\varepsilon_o) \sim 0.1$, regardless of ε_o. The maximum supersaturation for these parcels is very low, and under these conditions, perturbations in droplet number concentration result in dynamical readjustments in cloud maximum supersaturations that tend to maintain constant N. This variation in $\phi(\varepsilon_o)$ means that the importance of ε_o variability will depend on the cloud regime. The strongest surface tension effects are expected to be seen in cumulus and stratocumulus clouds, where updraft velocities are relatively high.

For the multimodal, continental aerosol shown in Fig. 4, $\phi(\varepsilon_o)$ increases with decreasing ε_o and increasing W for most of the parameter range. The $\phi(\varepsilon_o)$ values for typical continental conditions range from 0 to 0.2 in the
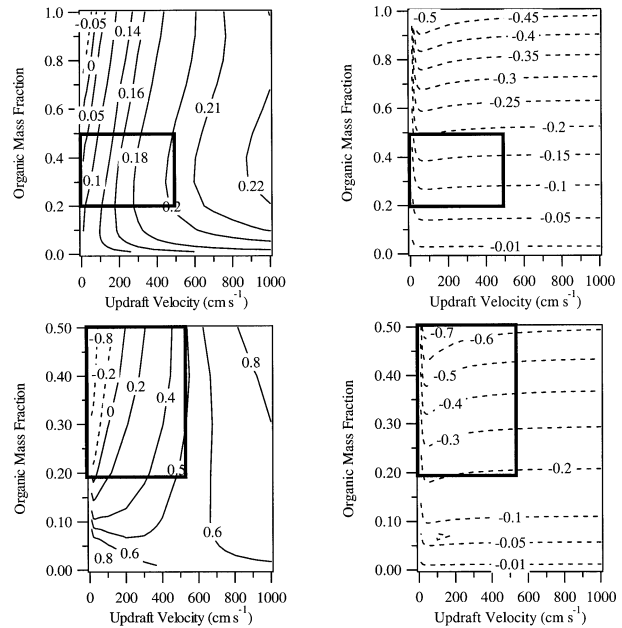

FIG. 4. Sensitivity ratio $\phi(\varepsilon_o)$ for a continental aerosol size distribution with (left) surface tension effects and (right) without surface tension effects. The aerosol consists of $(NH_4)_2SO_4$ and dissolved organics with (top) no insoluble species present and (bottom) 50% insoluble species. The inner rectangles represent typical organic mass fraction and updraft velocity ranges for stratocumulus clouds under continental conditions. Solid lines represent positive $\phi(\varepsilon_o)$ values; dashed lines represent negative $\phi(\varepsilon_o)$ values.

absence of insoluble species and from -2 to 0.5 when the insoluble mass fraction is 0.5 (both in the presence of surfactants). In the absence of surfactants, $\phi(\varepsilon_o)$ is negative and becomes larger as the organic mass fraction increases; this is expected, as the decreased hygroscopicity is most prominent when the CCN has a substantial amount of organics. Similar to what is seen under marine conditions, $\phi(\varepsilon_o)$ exhibits negative values at low W and high ε_o, which become larger in the presence of surfactants. Negative $\phi(\varepsilon_o)$ values are more prevalent for continental conditions as compared to marine conditions, because the higher concentration of aerosol decreases the maximum supersaturation even further for the same change in ε_o.

We note from Fig. 4 that there are areas of atmospheric relevance where $\phi(\varepsilon_o) \sim 0$, which generally occurs for low W and high ε_o (in the presence of surfactants) and low ε_o (in the absence of surfactant species). In these regions, the sensitivity of N to W is much greater than that of N to ε_o, and chemical effects can be negligible, or cancel out, particularly if the updraft velocity distribution is centered on a W for which $\phi(\varepsilon_o) \sim 0$.

For a given ε_o, $\phi(\varepsilon_o)$ increases with updraft velocity, as was seen under marine conditions in Fig. 3. However, under continental conditions, the asymptotic limit occurs for small updraft velocities ($W < 50$ cm s^{-1}) and the transition to the asymptotic regime is not as sharp
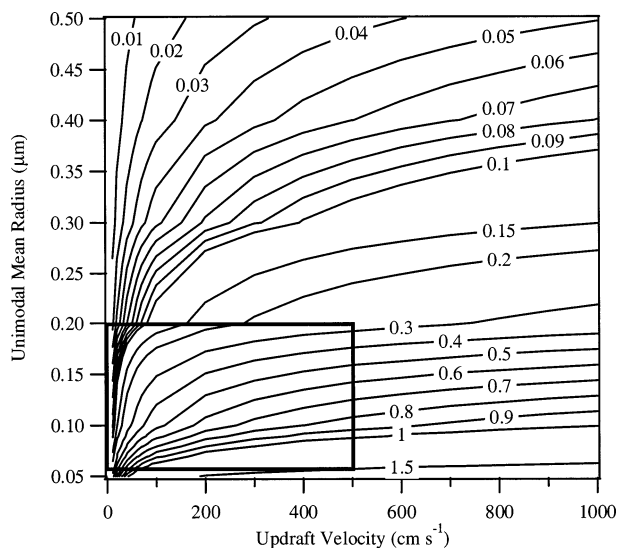
FIG. 5. Sensitivity ratio $\phi(a_m)$ for single-mode aerosol with $N_{ap} = 1000$ cm^{-3} and $\sigma = 2$. The aerosol is assumed to be composed of pure $(NH_4)_2SO_4$. The inner rectangle represents the typical unimodal mean radius and updraft velocity ranges for stratocumulus clouds under continental conditions. Solid lines represent positive $\phi(a_m)$ values.

as for marine conditions. For $W < 700$ cm s^{-1}, increases in ε_o lead to decreases in $\phi(\varepsilon_o)$; for $W > 700$ cm s^{-1}, increases in ε_o lead to increases in $\phi(\varepsilon_o)$. Again, the variation in the behavior of $\phi(\varepsilon_o)$ at constant W indicates that the importance of changes in ε_o depends on the cloud regime. As was seen under marine conditions, the strongest positive effects (in the presence of surfactants) are expected when updraft velocities are high.

A comparison between the $\phi(\varepsilon_o)$ values of Figs. 3 and 4 at particular values of W and ε_o further exemplifies this trend. For $W = 200$ cm s^{-1} and $\varepsilon_o = 0.3$, $\phi(\varepsilon_o)$ for marine conditions is about 0.38 in the absence of insoluble species and about 0.53 with an insoluble mass fraction of 0.5 (both in the presence of surfactants). For continental conditions, $\phi(\varepsilon_o)$ is about 0.16 in the absence of insoluble species and about 0.19 for an insoluble mass fraction of 0.5. Under these conditions, the presence of an insoluble species seems to have a small effect on droplet activation, which is consistent with a full activation model (Nenes et al. 2002a).

Figure 5 shows that $\phi(a_m)$ is largest for low W and a_m for a unimodal aerosol population, representative of a continental accumulation mode aerosol. The inner rectangle represents the ambient range of unimodal mean radius and organic mass fractions. Values of $\phi(a_m)$ in Fig. 5 vary from 0.01 to 1.5. The positive values of $\phi(a_m)$ result because the droplet number concentration is positively correlated with both updraft velocity and the geometric mean radius. The sensitivity of N with respect to a_m, although positive, decreases as a_m becomes larger. Thus, as a_m increases, $\phi(a_m) \to 0$. The high sensitivity of N to a_m results because a_m exerts a

strong effect on the shape of the CCN spectrum, which controls both the time at which the CCN start to absorb water as well as the maximum supersaturation achieved in the rising air parcel. In addition, N is less sensitive to large a_m than to small a_m. Particles with large radii activate for lower updraft velocities than those with small a_m. Whereas the activation fraction is relatively large with a large value for a_m, the differential change in N is small. With small a_m, the droplet number concentration tends to be smaller, and changes in the number activated will have a larger effect on total N.

Figure 6 shows $\phi(a_{mA})$, where the subscript A refers to the accumulation mode, for marine (top panel) and continental (bottom panel) aerosol size distributions. The inner rectangles represent the range of accumulation mode radius and organic mass fractions found in the atmosphere for marine and continental conditions, as reflected by measurements (e.g., Whitby 1978). The values for $\phi(a_{mA})$ vary from -0.6 to 0.3 for marine conditions and from -0.2 to 3.6 for continental conditions. When the aerosol size distribution is shifted toward smaller sizes, fewer CCN become activated in the initial stages of the cloud, and more water vapor is available for subsequent activation. By contrast, with a greater number of large particles present, the water vapor is absorbed earlier in the cloud resulting in less water vapor being available for subsequent particle growth. For this reason, $\phi(a_{mA})$ becomes negative for large a_{mA} and large updraft velocities. These results are consistent with those of Cohard et al. (1998, 2000).

For $W = 200$ cm s^{-1} and $a_{mA} = 0.1$ μm, $\phi(a_{mA})$ is about 0.02 for marine conditions and about 0.8 for continental conditions. Generally, cloud droplet formation is more sensitive to the geometric mean radius under continental conditions than under marine conditions. Since the total aerosol number concentration is larger for continental conditions than for marine conditions, the absolute number of activated droplets is also larger for continental conditions, and thus there is greater competition for water vapor among the particles.

4. Conclusions

The conditions under which chemical effects can either amplify or dampen the Twomey effect are assessed by determining relative sensitivities of different parameters, χ, to that of updraft velocity, W: $\phi(\chi) = (\chi/W)(\partial N/\partial \chi)/(\partial N/\partial W)$. Expressions for the sensitivity of N with respect to updraft velocity (W), aerosol number concentration (N_{ap}), organic mass fraction (ε_o), and geometric standard deviation (σ) and geometric mean radius (a_m) of the aerosol size distribution are derived for both unimodal and multimodal size distributions based on an extension of Köhler theory and the parameterization of Abdul-Razzak et al. (1998) and Abdul-Razzak and Ghan (2000) (Table 4). Both marine and continental conditions are studied.
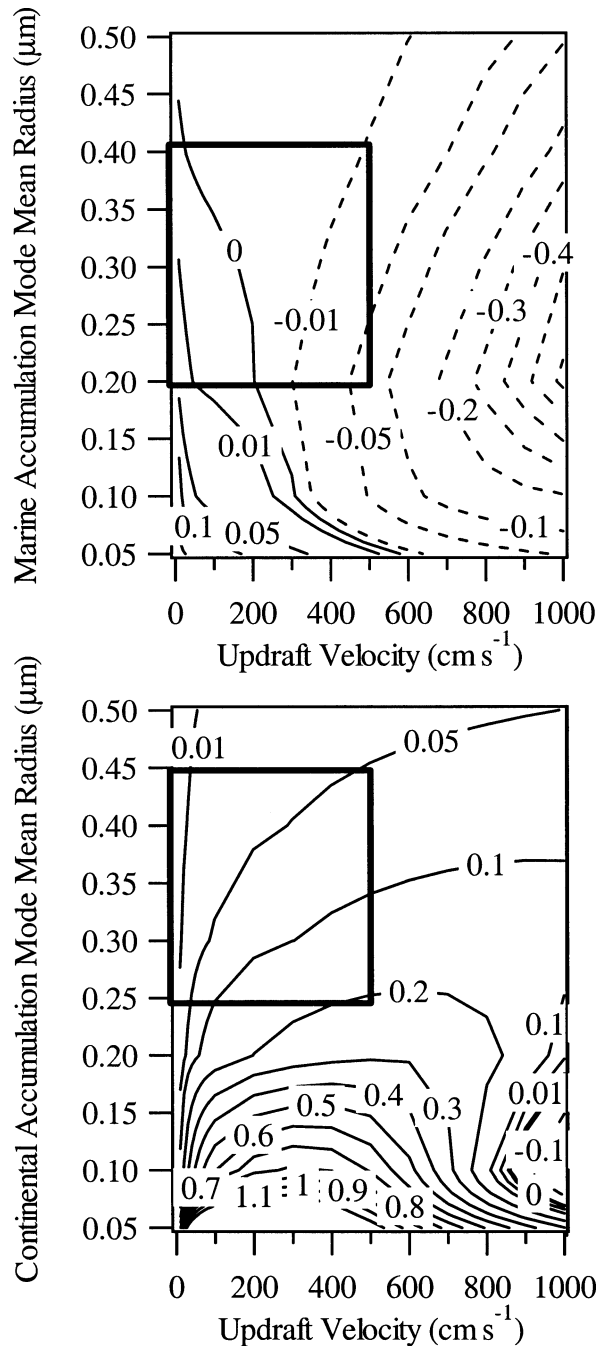
Although an increase in anthropogenic pollution (N_{ap})

FIG. 6. Sensitivity ratio $\phi(a_{mA})$: (top) marine and (bottom) continental aerosol size distribution. The aerosol is assumed to be composed of pure $(NH_4)_2SO_4$. The inner boxes represent typical accumulation mode mean radius and updraft velocity ranges for stratocumulus clouds under marine and continental conditions. Solid lines represent positive $\phi(a_m)$ values; dashed lines represent negative $\phi(a_m)$ values.

have two competing effects on cloud formation: (i) an increased number of CCN activated by increased N_{ap} and (ii), a decreased number of CCN activated by a greater presence of soluble organics. Consequently, regimes exist in which an increase in anthropogenic aerosol can actually lead to a decrease in cloud droplet number. The direction in which the presence of a soluble organic affects CCN activation will depend on the chemical characteristics of the aerosol, including its size distribution.

Chemical effects on cloud droplet number are complex, but not intractable. A range of computed sensitivity ratios show that chemical effects can, in some instances, be as influential as (or more influential than) variations in updraft velocity. Depending on atmospheric conditions, chemical effects can either enhance or weaken the activation process. An important finding is that, adding surfactants to the CCN drastically changes the character of the activation process; $\phi(\varepsilon_o)$ becomes a strong function of updraft velocity (this is not seen for the same aerosol in the absence of surfactants). This implies that, when studying aerosol–cloud interactions, the most influential (in terms of droplet number) updraft may not be in the peak of the probability distribution. Such insight is critical for understanding the aerosol indirect effect in both modeling studies and field experiments. Future work should focus on determining the range of solubility, hygroscopicity, and surfactant properties necessary to have an important effect on droplet number.

The results of the current study provide insight into the role of surface tension lowering organics on cloud properties on a global and single-cloud scale. On a global scale, the variability of both updraft velocities and soluble aerosol organic content can be used to identify regions for which organics can have the strongest influence on cloud properties (both positive or negative). On the scale of a single cloud, since one would not expect to see the variability in organic mass fraction that is seen on global scales, N is controlled primarily by dynamical conditions. The conditions for which variations in ε_o either magnify, diminish, or do not effect the variability of cloud droplet number concentration can be isolated from the variations caused by other quantities, such as aerosol number concentration and W.

One exception to this is in ship tracks. On the boundaries of such cloud systems, large variability in chemical composition can be seen. One can envision transitioning between a region where the additional CCN have no effect on cloud properties, $\phi(\varepsilon_o) \sim 0$; to a region where cloud droplet number concentration decreases, $\phi(\varepsilon_o) < 0$; to a region where cloud droplet number concentration increases, $\phi(\varepsilon_o) > 0$. Given that the meteorological conditions across ship track boundaries (i.e. updraft velocity distribution) are not expected to change appreciably, it is possible that changes can be primarily controlled by chemical effects, such as are illustrated here. The large variation in sign predicted for $\phi(\varepsilon_o)$ for polluted con-

leads to an increase in the number of cloud droplets formed, negative $\phi(\varepsilon_o)$ values are found for high ε_o, which is reflective of increasingly polluted conditions. Therefore, an increase in anthropogenic pollution can

ditions may help explain why cloud droplet number concentration is not always strongly correlated with CCN number in ship tracks.

REFERENCES

Abdul-Razzak, H., and S. J. Ghan, 2000: A parameterization of aerosol activation: 2. Multiple aerosol types. *J. Geophys. Res.,* **105,** 6837–6844.

——, ——, and C. Rivera-Carpio, 1998: A parameterization of aerosol activation: 1. Single aerosol type. *J. Geophys. Res.,* **103,** 6123–6131.

Cohard, J.-M., J.-P. Pinty, and C. Bedos, 1998: Extending Twomey's analytical estimate of nucleated cloud droplet concentrations from CCN spectra. *J. Atmos. Sci.,* **55,** 3348–3357.

——, ——, and K. Suhre, 2000: On the parameterization of activation spectra from cloud condensation nuclei microphysical properties. *J. Geophys. Res.,* **105** (D9), 11 753–11 766.

Facchini, M. C., M. Mircea, S. Fuzzl, and R. J. Charlson, 1999: Cloud albedo enhancement by surface-active organic solutes in growing droplets. *Nature,* **401,** 257–259.

Ghan, S. J., G. Guzman, and H. Abdul-Razzak, 1998: Competition between sea salt and sulfate particles as cloud condensation nuclei. *J. Atmos. Sci.,* **55,** 3340–3347.

Houghton, J. T., Y. Ding, D. J. Griggs, M. Noguer, P. J. Van der Linden, and D. Xiaosu, Eds., 2001: *Climate Change 2001: The Scientific Basis.* Cambridge University Press, 944 pp.

Junge, C. E., 1952: Die Konstitution der atmospherischen aerosols. *Ann. Meteor.,* **1,** 128–135.

Khvorostyanov, V. I., and J. A. Curry, 1999: A simple analytical model of aerosol properties with account for hygroscopic growth 1. Equilibrium size spectra and cloud condensation nuclei activity spectra. *J. Geophys. Res.,* **104** (D2), 2175–2184.

Nenes, A., and J. H. Seinfeld, 2003: Parameterization of cloud droplet formation in global climate models. *J. Geophys. Res.,* **108,** 4415, doi:10.1029/2002JD002911.

——, S. Ghan, H. Abdul-Razzak, P. Y. Chuang, and J. H. Seinfeld, 2001: Kinetic limitations on cloud droplet formation and impact on cloud albedo. *Tellus,* **53B,** 133–149.

——, R. J. Charlson, M. C. Facchini, M. Kulmala, A. Laaksonen, and J. H. Seinfeld, 2002a: Can chemical effects on cloud droplet number rival the first indirect effect? *Geophys. Res. Lett.,* **29,** 1848, doi:10.1029/2002GL015295.

——, W. C. Conant, and J. H. Seinfeld, 2002b: Black carbon radiative effects on cloud microphysics and implications for the aerosol indirect effect 2. Cloud microphysics. *J. Geophys. Res.,* **107,** 4605, doi:10.1029/2002JD002101.

Pruppacher, H. R., and J. D. Klett, 1997: *Microphysics of Clouds and Precipitation.* Kluwer Academic, 954 pp.

Seinfeld, J. H., and S. N. Pandis, 1998: *Atmospheric Chemistry and Physics.* John Wiley, 1326 pp.

Twomey, S., 1977: *Atmospheric Aerosols.* Elsevier, 302 pp.

Whitby, K. T., 1978: The physical characteristics of sulfur aerosols. *Atmos. Environ.,* **12,** 135–159.